Radiological Imaging

The Theory of Image Formation, Detection, and Processing

Volume 1

Harrison H. Barrett
William Swindell

Department of Radiology
and
Optical Sciences Center
University of Arizona
Tucson, Arizona

1981

ACADEMIC PRESS
A Subsidiary of Harcourt Brace Jovanovich, Publishers

New York London
Paris San Diego San Francisco
São Paulo Sydney Tokyo Toronto

Appendix C

Interaction of Photons with Matter

In this appendix we briefly review the interaction of x rays with matter. For more details the reader should consult a standard text such as Heitler (1966) or Evans (1968).

In Sections C.1–C.6 we consider matter in elemental form only. The extension to mixtures and compounds is outlined in Section C.7.

C.1 ATTENUATION, SCATTERING, AND ABSORPTION

When a primary x-ray beam passes through matter, it becomes weaker or attenuated as photons are progressively removed from it. This *attenuation* takes place by two competing processes: *scattering* and *absorption.* For our purposes, which involve diagnostic energy x rays and low-atomic-number elements, the distinction between scattering losses and absorption losses is clear. *Scattering losses* refer to the energy removed from the primary beam by photons that are redirected by (mainly Compton) scattering events. The energy is carried away from the site of the primary interaction. *Absorption losses* refer to the energy removed from the primary beam and transferred locally to the lattice in the form of heat. Absorbed energy is derived from the photoelectron in photoelectric interactions and from the recoil electron in Compton events. Energy that is lost from the primary flux by other than Compton scattered radiation may nevertheless ultimately appear as scattered radiation in the form of bremsstrahlung, *k*-fluorescence, or annihilation gamma rays.

C.1.1 Linear Attenuation Coefficient μ

A pencil beam of monochromatic photons in a homogeneous medium is attenuated according to Beer's law:

$$\Phi(x) = \Phi_0 \exp(-\mu x), \tag{C.1}$$

where Φ_0 is the incident photon fluence (photons per square centimeter), $\Phi(x)$ is the photon fluence after traveling distance x in the medium, and μ is the linear attenuation coefficient.

C.1.2 Mass Attenuation Coefficient (μ/ρ)

The mass attenuation coefficient (μ/ρ), defined by

$$\text{mass attenuation coefficient} = \text{linear attenuation coefficient/density} = (\mu/\rho), \tag{C.2}$$

is useful for calculating the mass of material required to attenuate a primary beam by a prescribed amount, i.e.,

$$\Phi(x)/\Phi_0 = \exp[-(\mu/\rho)x_m], \tag{C.3}$$

where x_m is the mass of attenuator per unit area of beam. The quantity x_m is simply ρx. It has typical dimensions of grams per square centimeter, while (μ/ρ) has dimensions of centimeters squared per gram. See also the comments on dose buildup at the end of this appendix.

C.1.3 Collision Cross Section σ

The attenuating material may be described by a volume density, n per cubic centimeter, of attenuating particles, each of which presents a cross-sectional area σ to the incident beam. A thin slab of material of thickness dx will thus remove a fraction $n\sigma\, dx$ of the incident photons from the beam:

$$-\frac{d\Phi}{\Phi} = n\sigma\, dx, \tag{C.4}$$

which integrates to Beer's law (C.1) if we make the formal substitution

$$\mu = \sigma n. \tag{C.5}$$

C.1.4 Competing Processes

In the energy range 10 keV to 100 meV, there are three principal ways in which the incident beam becomes attenuated. They are photoelectric ab-

sorption (n_a atoms/cm^3 with collision cross section σ^{pe} cm^2/atom), Compton collisions (n_e electrons/cm^3 with collision cross section σ^C), and pair production (n_a atomic nuclei/cm^3 with collision cross section σ^{pp}). Since σ can also be interpreted as the probability that a photon will be removed from the primary beam while it is passing through a layer of attenuating material containing one attenuating site per unit area (normal to the beam), we can write the *total atomic* cross section σ^{tot} for elements as

$$\sigma^{tot} = \sigma^{pe} + Z\sigma^C + \sigma^{pp}, \tag{C.6}$$

where Z is the atomic number.

We have assumed all electrons are free electrons and partake equally in Compton collisions, which is not strictly true, especially for heavy elements and low-energy x rays (see Section C.6). Note that σ^{pe} has been defined as the atomic cross section because the interaction is with the atom as a whole, not just the ejected electron.

Using (C.5), we write component parts to the linear and mass attenuation coefficients as follows:

$$\begin{aligned}(\mu/\rho)^{pe}\rho &= \mu^{pe} = n_a\sigma^{pe},\\ (\mu/\rho)^{C}\rho &= \mu^{C} = n_e\sigma^{C},\\ (\mu/\rho)^{pp}\rho &= \mu^{pp} = n_a\sigma^{pp},\end{aligned} \tag{C.7}$$

and the overall attenuation coefficients μ^{tot} and $(\mu/\rho)^{tot}$ are given by

$$\mu^{tot} = \sigma^{tot}n_a = \mu^{pe} + \mu^{C} + \mu^{pp} \tag{C.8}$$

and

$$(\mu/\rho)^{tot} = (\mu/\rho)^{pe} + (\mu/\rho)^{C} + (\mu/\rho)^{pp}. \tag{C.9}$$

C.2 PHOTOELECTRIC ABSORPTION

In a photoelectric event, the primary photon is destroyed. Its energy $h\nu_0$ ionizes the absorbing atom and imparts kinetic energy $\mathscr{E}_k$ to the ejected photoelectron. Conservation of energy requires that

$$h\nu_0 = \mathscr{E}_k + I, \tag{C.10}$$

where I is the ionization potential of the particular electron involved (see Fig. C.1). The deepest available atomic level always has the largest absorption cross section. A K-shell interaction is approximately four to five times more probable than an L-shell interaction if both interactions are energetically allowed.

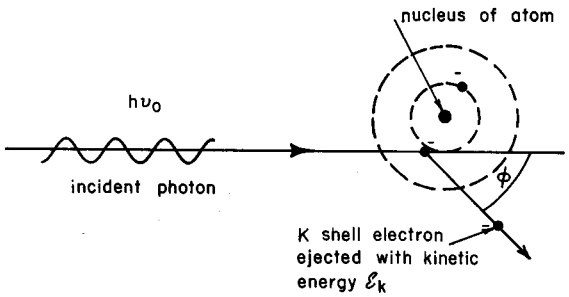

Fig. C.1 With photoelectric absorption, the incident photon is annihilated. Its energy is shared between ionizing the atom and imparting kinetic energy to the photoelectron.

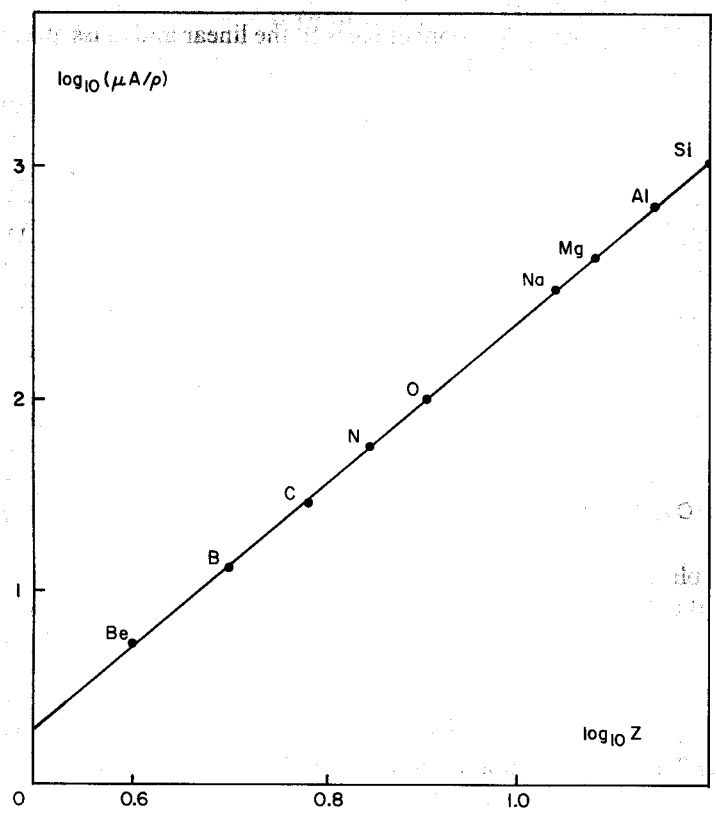

Fig. C.2 Using data from the Radiological Health Handbook (U.S. Department HEW, 1970) for 10-keV x rays, this graph justifies the choice $m = 4$ in (C.11). The slope is 4.13.

C.2.1 Dependence on Energy and Atomic Number

Experimentally it is found that the linear attenuation coefficient μ^{pe} is given by

$$\mu^{pe} \approx k \frac{Z^m}{(h\nu_0)^n} \frac{\rho}{A}, \tag{C.11}$$

where k is a constant that depends on the shell involved, ρ is the density, A the atomic weight, and Z the atomic number of the material. The parameters m and n are slowly varying functions of Z and ν_0, but a useful rule of thumb is obtained by writing

$$\mu^{pe} = k \frac{\rho}{A} \frac{Z^4}{(h\nu_0)^3}. \tag{C.12}$$

See, for example, Figs. C.2 and C.3.

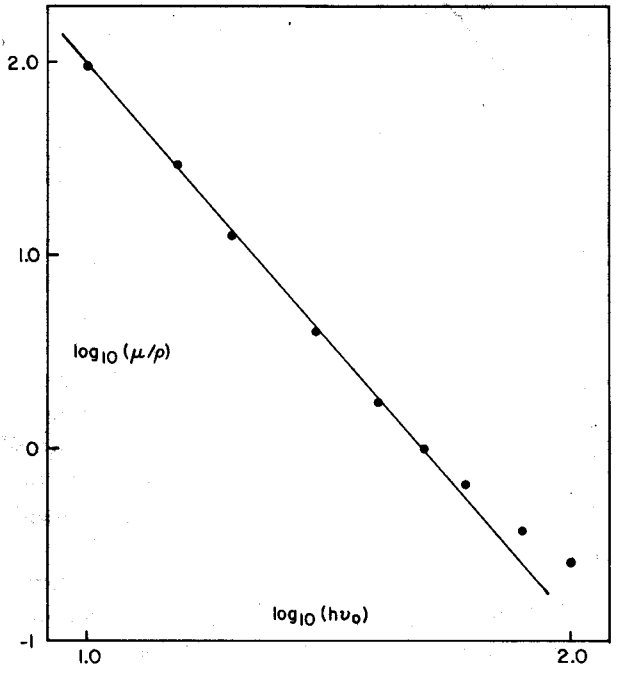

Fig. C.3 Using data from the Radiological Health Handbook (U.S. Department HEW, 1970) for calcium, this graph justifies the choice $n = 3$ in (C.11). Units of μ/ρ are square centimeters per gram and units of $h\nu_0$ are kilo-electron-volts. The photoelectric effect is dominant below 50 keV, in which region the linear fit is acceptable. The slope is 2.80.

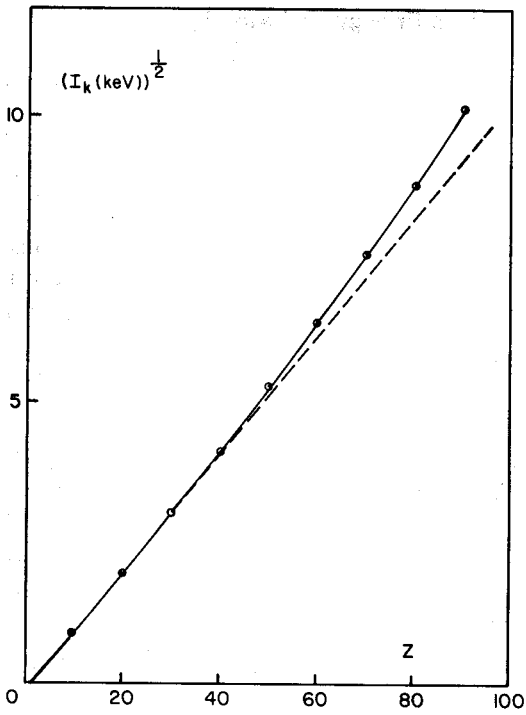

Fig. C.4 K-absorption edge is approximately proportional to Z^2. Data points for every tenth element ($Z = 10, 20, \ldots$) are shown.

C.2.2 Absorption Edges

A certain minimum primary photon energy I_K is required to ionize the K-shell electron. The position of this absorption edge is illustrated in Fig. C.4. As a very rough approximation, I_K is proportional to Z^2. Similar considerations apply to the L shell, except that there are several nondegenerate sublevels involved.

C.2.3 Angular Distribution of Photoelectrons

The number of photoelectrons d^2N_e scattered out of volume dV into solid angle $d\Omega$ in a direction ϕ with respect to the incident photon beam is given by

$$\frac{d^2N_e}{d\Omega\, dV} \propto \frac{\sin^2\phi}{[1-(v/c)\cos\phi]^4}, \tag{C.13}$$

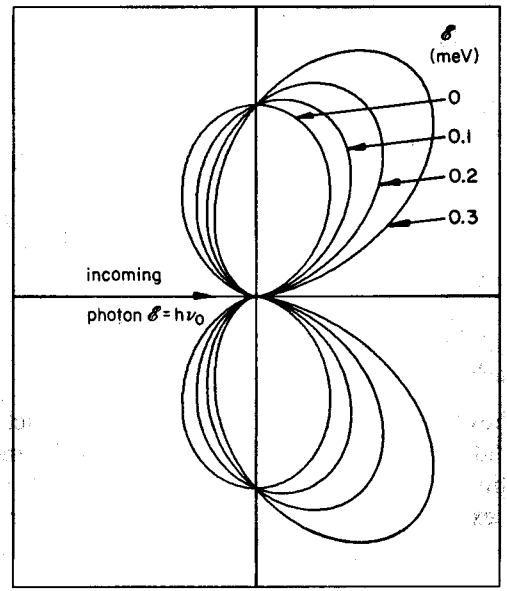

Fig. C.5 Angular distribution of emitted photoelectrons depends on the velocity of electron. The nonrelativistic expression (C.13) plotted here shows the dependence for an unpolarized photon stream.

where v is the velocity of the emitted photoelectron. This nonrelativistic expression assumes that the incoming photon beam is randomly polarized (see Fig. C.5). For polarized radiation, (C.13) has a factor $\cos^2 \phi_E$ in the numerator, where ϕ_E is the angle between the scattering plane and the electric field of the incident radiation.

C.3 COMPTON SCATTERING

C.3.1 Scattering Geometry

In a Compton event, the incoming photon with energy $h\nu_0$ is scattered by a free electron through angle θ. Energy $\mathscr{E}_k$ is imparted to the electron, which recoils at angle ϕ; the remaining energy $h\nu'$ stays with the scattered photon (see Fig. C.6).

With $\alpha = h\nu_0/m_0c^2$ ($m_0c^2 = 0.511$ meV), the energy of the scattered photon is given by

$$h\nu' = h\nu_0(1 + \alpha - \alpha\cos\theta)^{-1}. \tag{C.14}$$

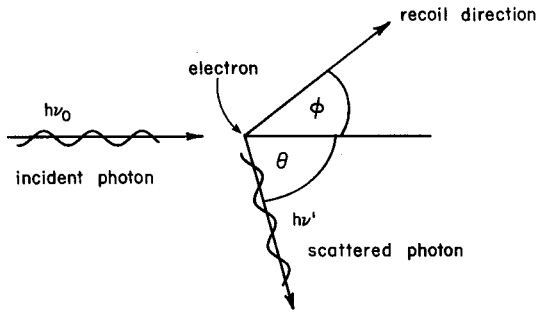

Fig. C.6 Geometry of Compton scattering.

Figure C.7 shows how the energy is divided as a function of primary photon energy and scattering angle. At diagnostic x-ray energies, most of the energy is retained by the scattered photon.

Other useful expressions relate the photon energies to the scattering angle,

$$\frac{1}{h\nu'} - \frac{1}{h\nu_0} = \frac{1}{m_0c^2}(1 - \cos\theta), \tag{C.15}$$

and the photon scattering angle θ to the electron recoil angle ϕ,

$$\cot\phi = (1 + \alpha)\tan(\theta/2). \tag{C.16}$$

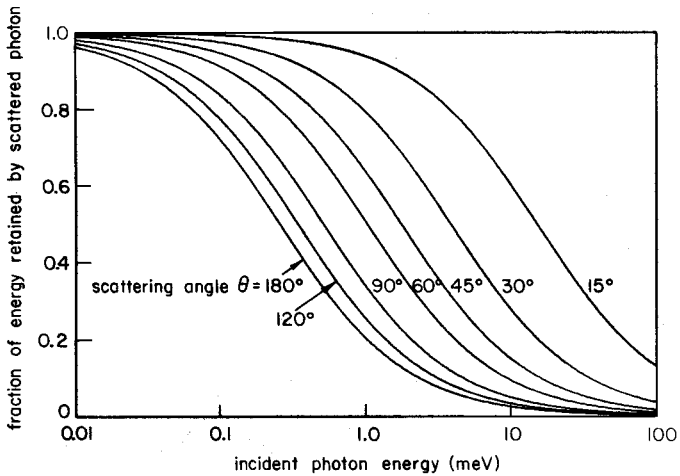

Fig. C.7 How the energy of the incident photon is divided between the scattered photon and the photoelectron.

The kinetic energy of the electron is given by

$$\mathscr{E}_k = hv_0\left[\frac{\alpha(1-\cos\theta)}{1+\alpha(1-\cos\theta)}\right]. \tag{C.17}$$

C.3.2 Collision Cross Section

The collision cross section σ^C determines the probability that an incident photon will undergo a Compton scatter. In a thin layer of thickness dx, we equate the probability of scattering with the fraction of the beam area that is occluded by the scattering sites, and it follows that

$$\text{probability of scatter} = -\frac{d\Phi}{\Phi} = n_e\sigma^C\,dx, \tag{C.18}$$

and the number of photons scattered per unit volume dN_s/dV is

$$\frac{dN_s}{dV} = -\frac{d\Phi}{dx} = \Phi n_e\sigma^C. \tag{C.19}$$

Similarly, the energy lost per unit volume from the primary beam is given by

$$w = -\frac{d\Psi}{dx} = \Phi hv_0 n_e\sigma^C, \tag{C.20}$$

where Ψ $(=\Phi hv_0)$ is the primary-beam energy fluence.

The expression for σ^C was first deduced by Klein and Nishina:

$$\frac{\sigma^C}{\sigma_0} = f_{KN}(\alpha) = \frac{3}{4}\left[\frac{2(1+\alpha)^2}{\alpha^2(1+2\alpha)} + \frac{\ln(1+2\alpha)}{\alpha}\left(\frac{1}{2} - \frac{1+\alpha}{\alpha^2}\right) - \frac{1+3\alpha}{(1+2\alpha)^2}\right], \tag{C.21}$$

where $\sigma_0 = 8\pi r_0^2/3$ is the cross section for (classical) Thomson scattering, and $r_0 = e^2/(m_0c^2) = 2.818 \times 10^{-13}$ cm. $f_{KN}(\alpha)$ is the Klein–Nishina function.

In terms of Avogadro's number N_0 $(=6.02 \times 10^{23}\ \text{mol}^{-1})$, the electron density n_e (cm^{-3}) is

$$n_e = N_0\rho Z/A. \tag{C.22}$$

If we assume that all atomic electrons participate in Compton scattering equally, then using (C.5) we can write

$$(\mu/\rho)^C = \sigma^C(N_0Z/A). \tag{C.23}$$

Thus the mass attenuation coefficient $(\mu/\rho)^C$ due to the Compton process depends only on Z/A (in addition to the energy dependence). For all but the lightest elements, $Z/A \approx 0.5$. Therefore, almost all matter has essentially the same Compton mass attenuation coefficient.

The linear (Compton) attenuation coefficient is given by

$$\mu^C = \sigma^C \rho N_0 Z/A = (\sigma_0 \rho N_0 Z/A) f_{KN}(\alpha). \tag{C.24}$$

The energy density w removed from the primary beam as given by (C.20) can be resolved into two components,

$$w = w_s + w_{en}, \tag{C.25}$$

where w_s is the energy per unit volume that appears as scattered radiation and w_{en} is the energy per unit volume that is imparted as kinetic energy to the recoil electrons. By analogy with (C.20), the scattering cross section σ_s^C is defined by

$$w_s = \Phi h\nu_0 n_e \sigma_s^C. \tag{C.26}$$

Since $\Psi = \Phi h\nu_0$, this equation can be rewritten

$$w_s = \Psi n_e \sigma_s^C. \tag{C.27}$$

The scattering cross section is given by [Evans (1968)]

$$\sigma_s^C = \frac{3}{8}\sigma_0\left(\frac{2(2\alpha^3 - 3\alpha - 1)}{\alpha^2(1+2\alpha)^2} + \frac{8\alpha^2}{3(1+2\alpha)^3} + \frac{\ln(1+2\alpha)}{\alpha^3}\right). \tag{C.28}$$

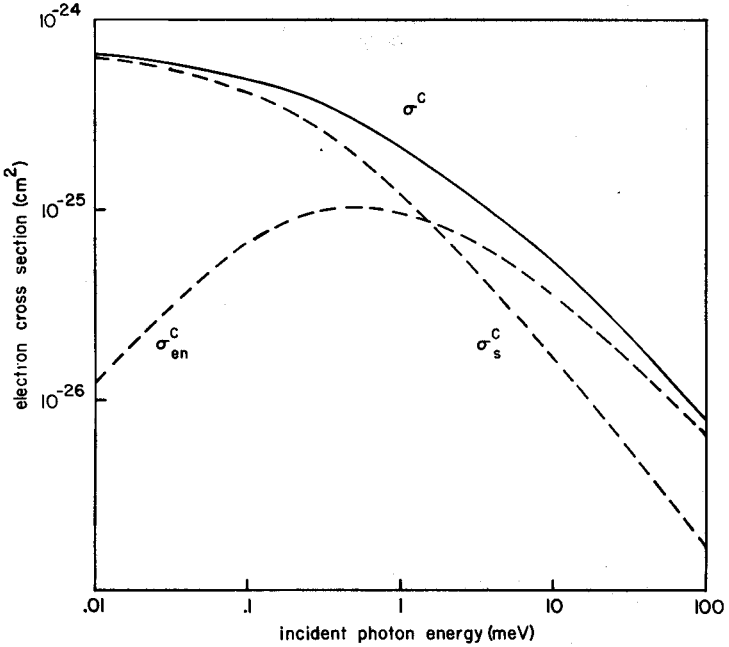

Fig. C.8 Klein–Nishina cross sections for a free-electron Compton interaction.

Similarly, the absorption cross section σ_{en}^{C} determines the energy absorbed per unit volume by the recoil electrons, w_{en};

$$w_{en} = \Psi n_e \sigma_{en}^{C}, \tag{C.29}$$

which can also be written

$$w_{en} = \Phi h\nu_0 n_e \sigma_{en}^{C} \tag{C.30}$$

Using (C.20), (C.25), (C.27), and (C.29), it follows at once that

$$\sigma_{en}^{C} = \sigma^{C} - \sigma_s^{C}, \tag{C.31}$$

which can be evaluated using (C.21) and (C.28). The energy dependences of σ^{C}, σ_s^{C}, and σ_{en}^{C} are shown in Fig. C.8.

C.3.3 Differential Cross Sections

The *differential cross sections* are useful because they permit the calculation of the angular distribution of the various quantities involved. The *collision differential cross section* $(d\sigma^{C}/d\Omega)_\theta$ is defined such that $d\sigma^{C}$ is the probability that an incident photon will be deflected into the elemental solid angle $d\Omega$ when passing through an attenuator containing one scattering center per unit area. If the radiation is unpolarized, the collision differential cross section $(d\sigma^{C}/d\Omega)_\theta$ depends only on θ, the angle of deflection of the photon. Thus it follows that σ^{C} and $(d\sigma^{C}/d\Omega)_\theta$ are related by

$$\sigma^{C} = \int_0^{\pi} \left(\frac{d\sigma^{C}}{d\Omega}\right)_\theta 2\pi \sin\theta \, d\theta. \tag{C.32}$$

An equivalent definition is given by differentiating (C.19) with respect to Ω:

$$\left[\frac{d^2 N_s}{dV\, d\Omega}\right]_\theta = \Phi n_e \left(\frac{d\sigma^{C}}{d\Omega}\right)_\theta, \tag{C.33}$$

where d^2N_s is the number of photons scattered into $d\Omega$ from volume element dV for incident fluence Φ (see Fig. C.9).

The collision differential cross section is given by

$$\left(\frac{d\sigma^{C}}{d\Omega}\right)_\theta = \frac{r_0^2}{2}\left(1 + \frac{\alpha^2(1-\cos\theta)^2}{(1+\cos^2\theta)[1+\alpha(1-\cos\theta)]}\right)\frac{1+\cos^2\theta}{[1+\alpha(1-\cos\theta)]^2}. \tag{C.34}$$

There are two useful ways to display this result, as shown in Figs. C.10 and C.11. It is interesting to note that the forward ($\theta = 0$) scattering properties of a given material are independent of incident photon energy.

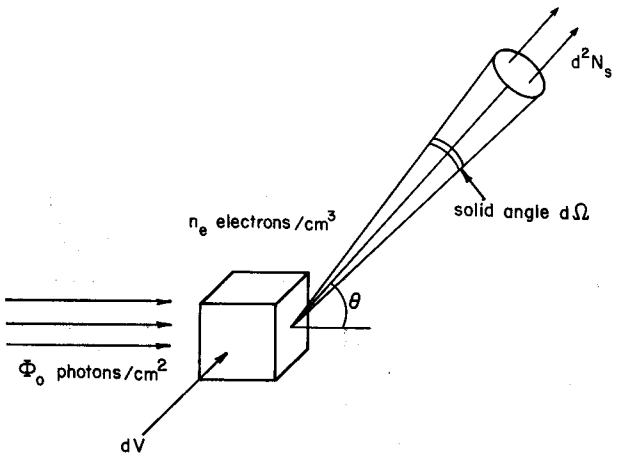

Fig. C.9 Number of photons d^2N_s scattered into solid angle $d\Omega$ from volume element dV is determined by the differential cross section. See (C.33).

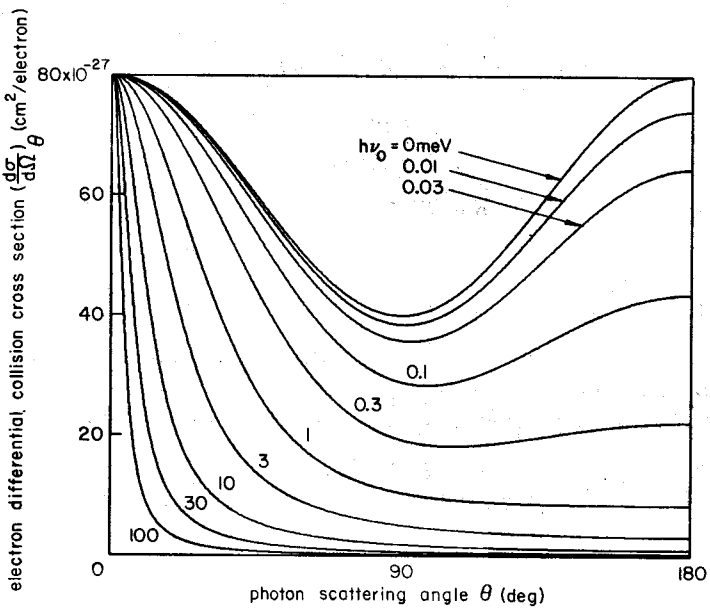

Fig. C.10 Differential collision cross section for free electrons.

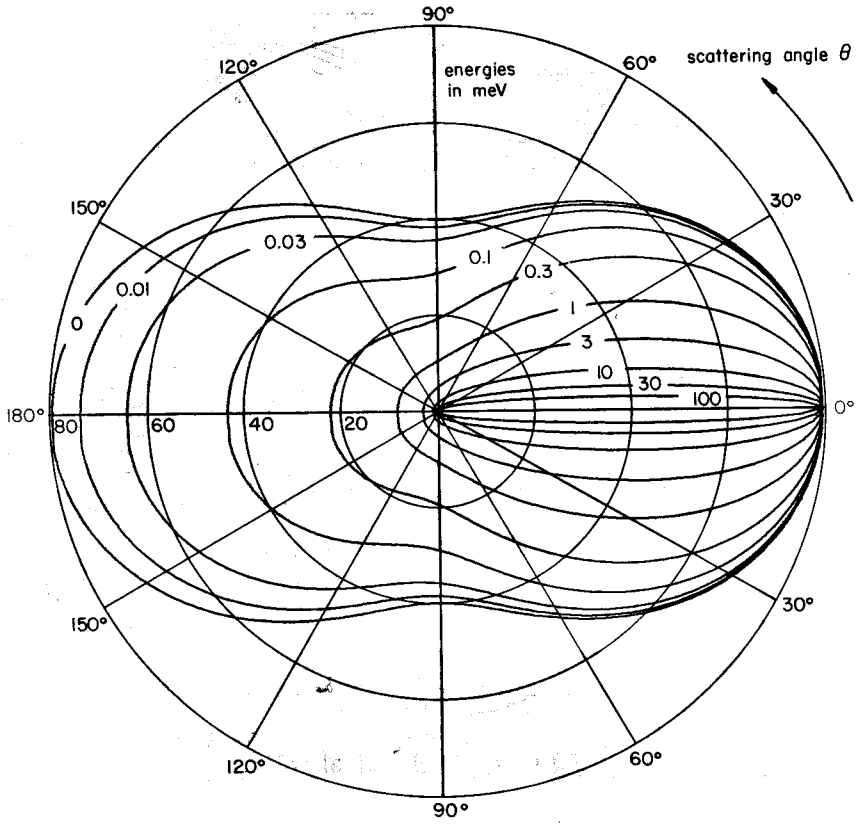

Fig. C.11 Differential collision cross section for free electrons is shown here in polar form. The units are 10^{-27} cm^2/steradian-electron.

Occasionally, one is interested in the number of photons scattered into a forward cone of semiangle θ_c from a scattering volume dV. This number, dN_s, is given by

$$\left[\frac{dN_s}{dV}\right]_{\theta<\theta_c} = \Phi n_e \int_0^{\theta_c} \frac{d\sigma^C}{d\Omega} 2\pi \sin\theta \, d\theta. \tag{C.35}$$

The normalized conical scattering fraction $f^C_{\theta_c}$, where

$$f^C_{\theta_c} = \frac{\int_0^{\theta_c} (d\sigma^C/d\Omega) 2\pi \sin\theta \, d\theta}{\int_0^{\pi} (d\sigma^C/d\Omega) 2\pi \sin\theta \, d\theta}, \tag{C.36}$$

is shown in Fig. C.12.

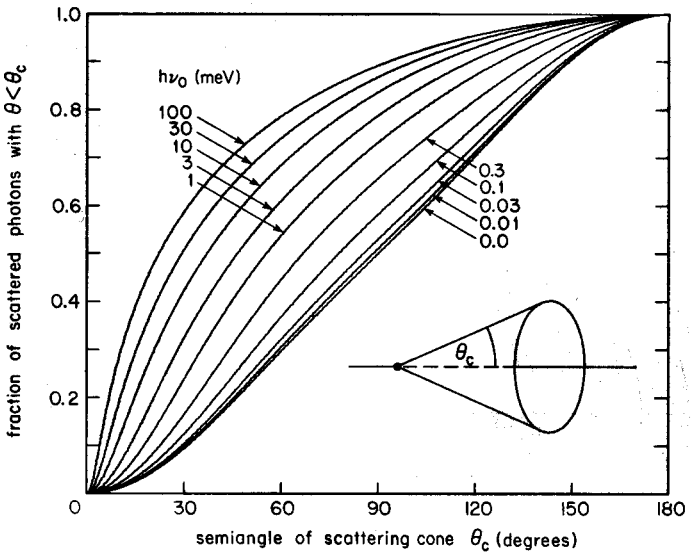

Fig. C.12 Ratio of the number of all photons that are scattered into a cone of semiangle θ_c about the direction of the incident beam to the total number scattered is shown as a function of primary beam energy.

We next determine the amount of *energy* $d^2\mathscr{E}_s$ that is scattered into an elementary solid angle $d\Omega$ from the elemental volume dV. It follows from (C.33) that this energy is given by

$$\left[\frac{d^2\mathscr{E}_s}{dV\,d\Omega}\right]_\theta = h\nu'\Phi n_e\left(\frac{d\sigma^C}{d\Omega}\right)_\theta, \tag{C.37}$$

and we can define the *scattering differential cross section* $(d\sigma_s^C/d\Omega)_\theta$ by

$$\left[\frac{d^2\mathscr{E}_s}{dV\,d\Omega}\right]_\theta = h\nu_0\Phi n_e\left(\frac{d\sigma_s^C}{d\Omega}\right)_\theta. \tag{C.38}$$

Thus,

$$\left(\frac{d\sigma_s^C}{d\Omega}\right)_\theta = \frac{\nu'}{\nu_0}\left(\frac{d\sigma^C}{d\Omega}\right)_\theta = [1+\alpha(1-\cos\theta)]^{-1}\left(\frac{d\sigma^C}{d\Omega}\right)_\theta. \tag{C.39}$$

This quantity is shown in Fig. C.13. Equations (C.34) and (C.38) can be used to compute the angular distribution of scattered photon energy.

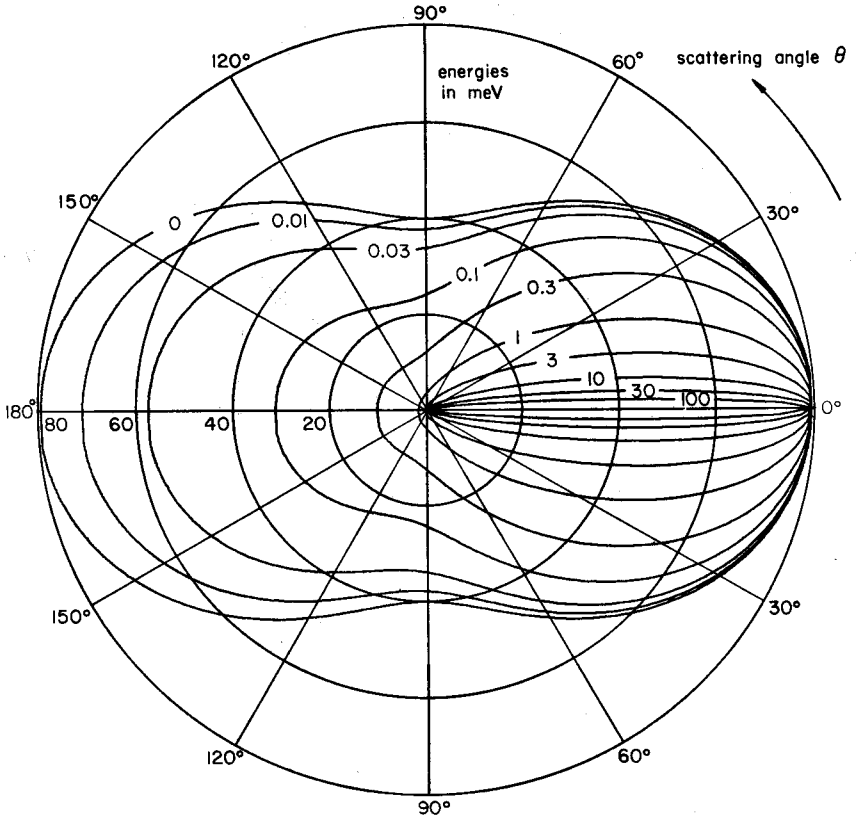

Fig. C.13 Scattering differential cross section, which describes the angular distribution of scattered energy, is shown as a function of primary beam energy. The units are 10^{-27} cm^2/steradian-electron.

C.3.4 The Compton Recoil Electron

There is a direct correspondence between the angle of the scattered photon and the angle ϕ of the recoil electron trajectory. Thus the number of recoil electrons ejected per unit solid angle per unit volume is given by (C.33), suitably modified to account for the solid angle rescaling:

$$\left[\frac{d^2N_e}{dV\,d\Omega}\right]_\phi = \Phi n_e \left(\frac{d\sigma^C}{d\Omega}\right)_\theta \frac{d\theta}{d\phi}\frac{\sin\theta}{\sin\phi}, \tag{C.40}$$

where θ and ϕ are related through (C.16). The angular dependence of this quantity is shown in Fig. C.14.

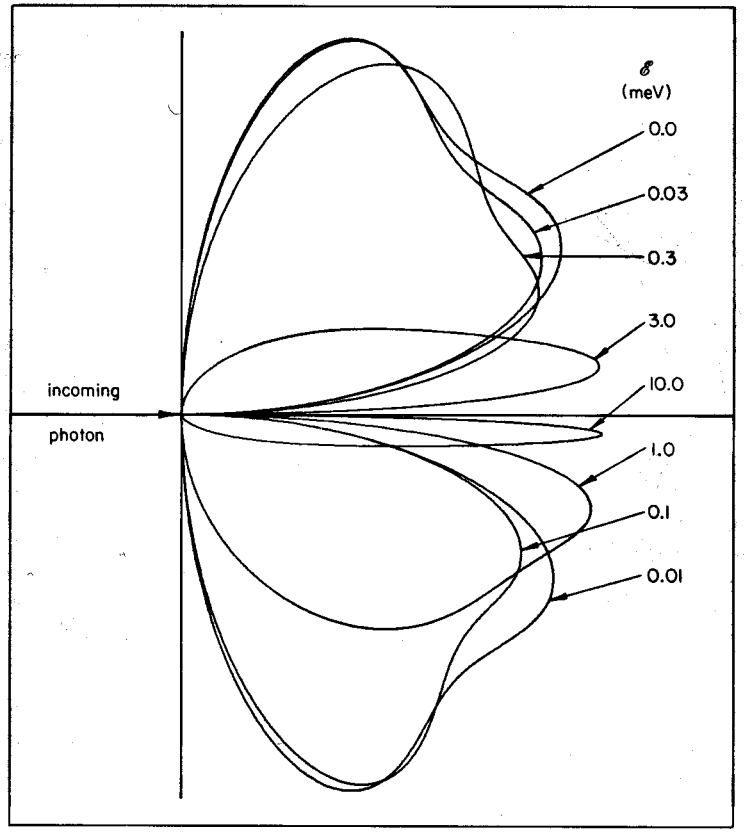

Fig. C.14 Quantity $(d\sigma^C/d\Omega)_\theta(d\theta/d\phi)\sin\theta/\sin\phi$ is proportional to the number of recoil electrons per unit solid angle centered on a direction at angle ϕ with the incident radiation. In this plot the polar angle is ϕ.

C.4 PAIR PRODUCTION

For incident photons of energy $h\nu_0 > 1.02$ meV, there is a probability of photon annihilation in the field of an atomic nucleus. There is the simultaneous creation of an electron and a positron, where the total kinetic energy $\mathscr{E}_{e-} + \mathscr{E}_{e+}$ is the difference between $h\nu_0$ and the particle rest masses, 1.02 meV:

$$h\nu_0 = 1.02 + \mathscr{E}_{e+} + \mathscr{E}_{e-} \quad \text{meV}. \tag{C.41}$$

The kinetic energy of either particle is continuously variable from zero to the maximum possible as stated above. The atomic collision cross section

for pair production varies approximately as Z^2 and increases monotonically with energy at least up to energies of 100 meV.

C.5 TOTAL ATTENUATION COEFFICIENT

From the previous discussion, it is apparent that the Compton linear attenuation coefficient μ^C can be written as the sum of two components μ_s^C and μ_{en}^C, where the subscripts s and en refer to photons (or energy) removed from the primary beam by the scattered radiation and by absorption. Therefore (C.8) can be written

$$\mu^{tot} = \mu^{pe} + \mu_{en}^C + \mu^{pp} + \mu_s^C. \tag{C.42}$$

The first three terms refer to the transfer of energy to the medium, while the fourth refers to scattered energy. It is common practice to combine the absorption terms into a total absorption term μ_{abs} and regard the total attenuation as the sum of a total absorption and a scattering term (see Fig. C.15).

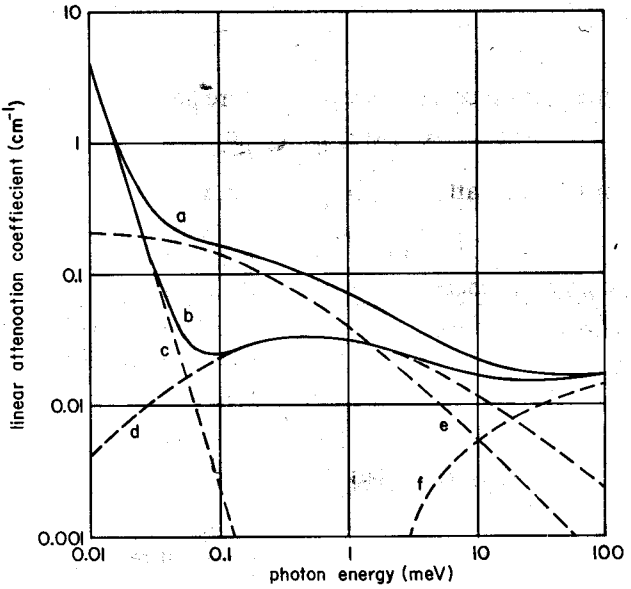

Fig. C.15 Total linear attenuation coefficient of water is the sum of three linear absorption coefficients and the Compton scattering coefficient: (a) Total linear attenuation coefficient, μ^{tot}; (b) Total absorption coefficient $\mu^{PE} + \mu_{en}^C + \mu^{PP}$; (c) Absorption coefficient for photoelectric processes, μ^{PE}; (d) Compton absorption coefficient μ_{en}^C. (e) Compton scattering coefficient μ_s^C. (f) Absorption coefficient for pair production μ^{PP}.

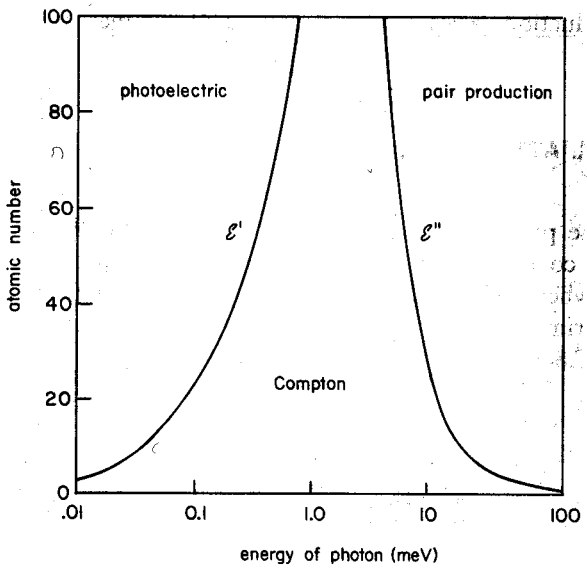

Fig. C.16 Curves $\mathscr{E}'$ and $\mathscr{E}''$ define the regions in which the various attenuation processes are dominant.

The linear attenuation coefficient can therefore be written

$$\mu^{\text{tot}} = \mu_{\text{abs}} + \mu_s^{\text{C}}. \tag{C.43}$$

Similarly, for the mass attenuation coefficient, we have

$$(\mu^{\text{tot}}/\rho) = (\mu_{\text{abs}}/\rho) + (\mu_s^{\text{C}}/\rho). \tag{C.44}$$

For each element, there is a particular energy $\mathscr{E}'$ for which $\mu^{\text{pe}} = \mu^{\text{C}}$ and another energy $\mathscr{E}''$ for which $\mu^{\text{C}} = \mu^{\text{pp}}$. These energies are plotted as a function of Z in Fig. C.16 to illustrate the regimes over which each attenuating process is dominant.

C.6 OTHER CONSIDERATIONS

The absorption processes we have discussed all result in the creation of moving electrons and, for the photoelectric effect, fluorescent x rays, so the site at which energy is removed from the beam is not necessarily the site at which it is deposited in the attenuator.

Fluorescent x rays have energies below the absorption edge of the shell that was ionized by the primary radiation. There is a reasonable chance that

they will escape the region of interest (K escape) because of the reduced attenuation coefficients for energies just below the absorption edge.

High-speed electrons communicate energy to the lattice of the attenuator by collision processes. Most of the energy gets delivered toward the end of the electron path, the path length itself being rather hard to define because of the statistical variations. However, to a good degree of approximation the range depends only upon the electron density of the absorber and the initial kinetic energy of the moving electron. A single curve of range ~~(cm)/ρ(gm/cm³)~~ gm/cm2 versus energy is sufficient to indicate the range over which the absorbed energy is spread by the energetic electrons (see Fig. C.17).

Beer's law only holds for a pencil beam geometry where the scattered radiation is completely removed from the main beam. With a wide beam, much of the scattered radiation carries on with a forward component to its

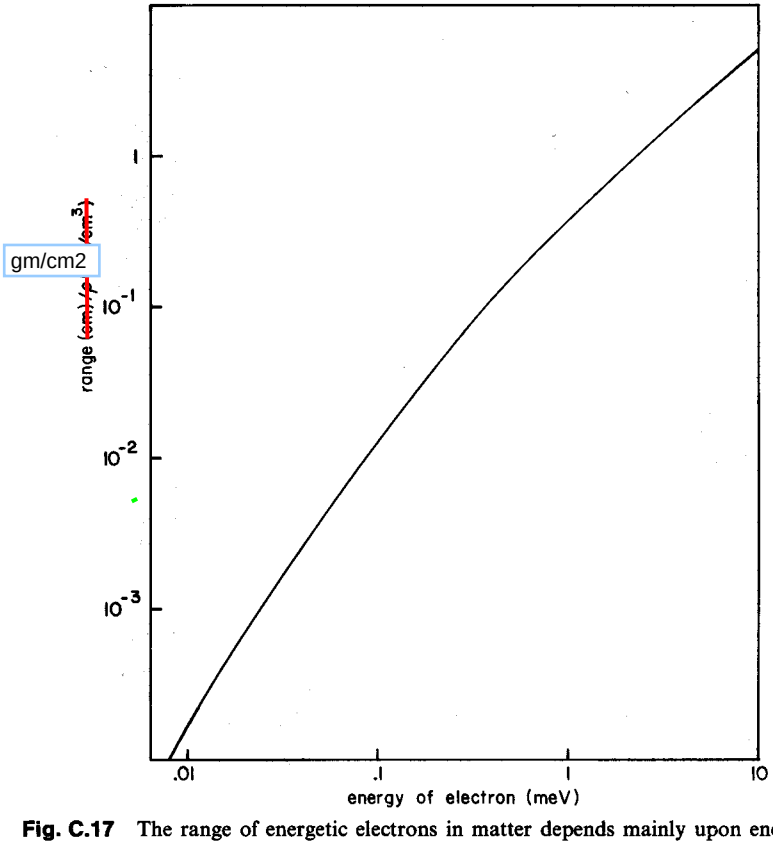

Fig. C.17 The range of energetic electrons in matter depends mainly upon energy and electron density in the attenuator. This universal curve serves to indicate the approximate range.

direction and will eventually leave the attenuating material superimposed on the main beam, even though not traveling in precisely the same direction. Thus, if a slab of material is used for shielding purposes, it is incorrect simply to apply Beer's law to calculate its attenuation factor. This would predict a shielding factor lower than would be observed in practice. There are tables of "Dose Buildup Factor" readily available (see, e.g., U.S. Department HEW, 1970) which permit the shielding properties of material slabs to be evaluated.

With regard to the Compton effect, we have assumed that all electrons in the scattering material are free. For most biological materials $I_K < 500$ eV, and very little of the incident photon energy is expended in ionizing any of the atomic electrons. At very low incident energies with high-Z materials, the K-shell electrons may be too tightly bound to participate. But this is precisely where the photoelectric absorption dominates the attenuation processes. In practice, there is no appreciable error in using the Klein–Nishina theory to determine the Compton contribution to the overall attenuation process.

C.7 MIXTURES AND COMPOUNDS

Chemical binding energies are so small compared to x-ray energies of interest that chemical compounds may be treated as mixtures. The mass attenuation coefficient for a mixture that consists of I components, each with mass attenuation coefficient $(\mu/\rho)_i$, $i = 1, \ldots, I$ is given by

$$\left(\frac{\mu}{\rho}\right) = \sum_{i=1}^{I} \left(\frac{\mu}{\rho}\right)_i W_i, \tag{C.45}$$

where W_i is the fraction by weight of the ith component. The linear attenuation coefficient is obtained by multiplying both sides of (C.45) by the density of its mixture.